SCIENCE CHINA
Information Sciences

• RESEARCH PAPER •

April 2022, Vol. 65 142403:1–142403:7
https://doi.org/10.1007/s11432-020-3244-8

Femtosecond laser-assisted switching in perpendicular magnetic tunnel junctions with double-interface free layer

Luding WANG[1,2], Wenlong CAI[1], Kaihua CAO[1], Kewen SHI[1], Bert KOOPMANS[2*] & Weisheng ZHAO[1*]

[1]*Fert Beijing Institute, School of Integrated Circuit Science and Engineering, Beihang University, Beijing* 100191*, China;*
[2]*Department of Applied Physics, Institute for Photonic Integration, Eindhoven University of Technology, Eindhoven* 5600 MB*, The Netherlands*

Received 7 December 2020/Revised 16 January 2021/Accepted 4 March 2021/Published online 26 November 2021

Abstract Perpendicular magnetic tunnel junctions with double-interface free layer (p-DMTJs), which exhibit enhanced tunnel magnetoresistance (TMR) and thermal stability (Δ) at the nanoscale, have received considerable interest as building blocks for spintronic data storage devices. Heat-assisted magnetic recording (HAMR) techniques have been widely employed in mainstream magnetic storage to enable ultrahigh storage density. However, the data access is achieved by sensing the stray field of the selected magnetic element using a mechanical "read head", resulting in an unfavorable speed limitation and design complexity. To address this issue, integrating laser-assisted switching with a high-performance magnetic tunnel junction has received interest in spintronic R&D; however, it has not yet been achieved. In this study, we experimentally explored femtosecond (fs) laser-assisted switching in a p-DMTJ device using a direct electrical TMR readout. We demonstrate two reconfigurable switching operations, i.e., binary "write" and unidirectional "reset", by the interplay of the fs laser and synchronized magnetic field sequence. We further explored the joint effect, and a switching phase diagram was obtained. The effect of the stray field of p-DMTJ, as well as laser helicity, on switching is also discussed. Results show the feasibility of fs laser-assisted writing p-DMTJs, which can pave the way in high-density optospintronic storage applications.

Keywords magnetic tunnel junctions (MTJs), heat-assisted magnetic recording (HAMR), spintronics, femtosecond laser, thermally-assisted switching (TAS)

Citation Wang L D, Cai W L, Cao K H, et al. Femtosecond laser-assisted switching in perpendicular magnetic tunnel junctions with double-interface free layer. Sci China Inf Sci, 2022, 65(4): 142403, https://doi.org/10.1007/s11432-020-3244-8

1 Introduction

The emerging potentials of magnetic tunnel junctions (MTJs) as building blocks for next-generation spintronic data storage devices have attracted significant attention owing to their nonvolatility and high scalability [1–7]. CoFeB/MgO-based MTJs with perpendicular magnetic easy axis (p-MTJs), where perpendicular magnetic anisotropy (PMA) originates at the CoFeB/MgO interface [8], have high thermal stability (Δ) for nanoscale devices, high tunnel magnetoresistance ratio (TMR), and low power consumption simultaneously [9–11]. Recently, it was reported that TMR and Δ can be further increased in p-MTJs using a MgO/CoFeB/W/CoFeB/MgO double-interface free layer (FL) structure (p-DMTJs) [12,13] with atom-thick W spacer and bridging layers [14–16]. This offers a suitable candidate to facilitate high-performance spintronic data storage [17].

As to mainstream magnetic storage, such as hard disc drives, heat-assisted magnetic recording (HAMR) techniques have been widely employed to enhance storage density [18,19]. In a HAMR device, switching is assisted by the local laser heating of the magnetic element, which momentarily lowers its coercive field.

* Corresponding author (email: b.koopmans@tue.nl, weisheng.zhao@buaa.edu.cn)

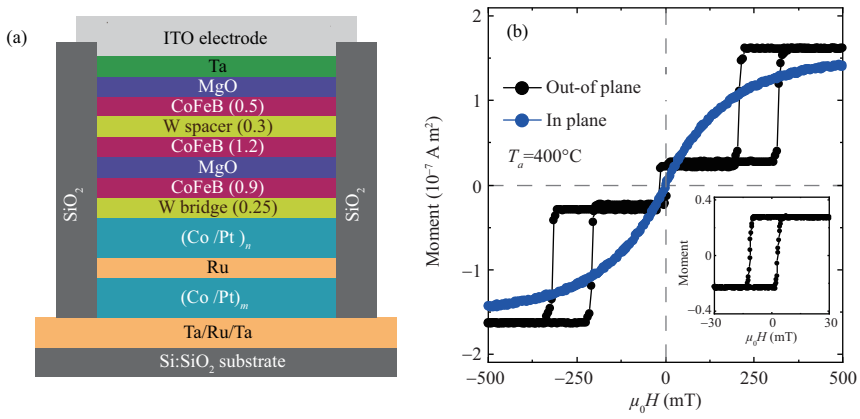

Figure 1 (Color online) MTJ stack structure and magnetic characteristics. (a) Schematic of the p-DMTJ stack structure. Ta/Ru/Ta is the bottom electrode. The bottom $(Co/Pt)_m$ and top $(Co/Pt)_n$ with the CoFeB layer were antiferromagnetically coupled with a thin Ru layer to form a SAF reference layer. The MgO layer is the tunnel barrier. The double-free-layer structure (CoFeB/W/CoFeB/MgO) with an atom-thick W spacer was used. (b) *M*-*H* hysteresis loops measured as a function of out-of-plane (black) and in-plane (blue) applied magnetic field at room temperature using PPMS-VSM. The film exhibited strong PMA in both the free and reference layers. Inset: Out-of-plane *M*-*H* minor loop of the p-DMTJ stack.

Moreover, a reduced magnetic field is generated by the "write head" to set the magnetization direction. Nevertheless, as to data access, a mechanical "read head" is always required to sense the stray field or magnetic-optical contrast of the selected magnetic element, which results in an unfavorable access delay and design complexity.

To address this issue, integrating heat-assisted switching with MTJs has been considerably investigated in spintronic R&D [20], such as thermally-assisted switching (TAS) schemes [21,22]. By circulating current in write lines, Joule heating has been used to assist the switching of specially designed in-plane MTJs while a reduced magnetic field is applied. However, current-induced Joule heating unavoidably results in drastic energy dissipation and heat-up delay. For future high-density spintronic storage [23, 24], the femtosecond (fs) laser-assisted switching of a high-performance p-DMTJ has not yet been proposed. The effect of additional magnetic FLs on the switching process has not been clarified. Moreover, no systematic study has been reported on the joint effect of laser and synchronized magnetic fields.

In this work, we experimentally investigated fs laser-assisted switching in a high-performance p-DMTJ device, which was read out directly through a real-time electrical TMR measurement. Using an fs laser pulse train and a synchronized magnetic field sequence, reconfigurable switching operations, such as the toggle "write" and unidirectional "reset", were investigated. The synergy between the fs laser pulses and the magnetic field sequence was further investigated, and a switching phase diagram was obtained. Finally, the effect of the stray field of p-DMTJ, as well as laser helicity, on switching is discussed.

2 Device characterization

Figure 1(a) shows a magnetic thin film of the p-DMTJ used in this study. This film comprises, from the substrate side upwards, Ta (3)/Ru (20)/Ta (0.7)/$[Co\ (0.5)/Pt\ (0.35)]_6$/Co (0.6)/Ru (0.8)/Co (0.6)/$[Pt\ (0.35)/Co\ (0.5)]_3$/W (0.25)/CoFeB (0.9)/MgO (0.8)/CoFeB (1.2)/W (0.3)/CoFeB (0.5)/MgO (0.8)/Pt (1.5), deposited on a thermally oxidized Si (001) substrate at room temperature (30°C) through Singulus DC and RF magnetron sputtering (numbers in parentheses denote the thicknesses of each layer in nanometers, and the subscripts for Co/Pt multilayers are the numbers of repeat). The composition of the CoFeB target was $Co_{20}Fe_{60}B_{20}$ (in atomic %). The Ta/Ru/Ta layer was used as the bottom electrode. The bottom $(Co/Pt)_m$ and top $(Co/Pt)_n$ multilayers, with the CoFeB layer, were antiferromagnetically coupled through a thin Ru layer, forming a synthetic antiferromagnetic (SAF) reference layer. The MgO layer was the tunnel barrier. For the FL, the bottom and top CoFeB layers were ferromagnetically coupled with a 0.3-nm W spacer layer. The double-FL structure was employed to enhance Δ while maintaining the writing energy efficiency. After deposition, the stacks were annealed at 400°C in a vacuum for 1 h to enhance PMA.

We investigated the magnetic characteristics of the full-sheet MTJ stack using physical properties measurement system-vibrating sample magnetometer (PPMS-VSM) at room temperature (30°C). Figure 1(b)

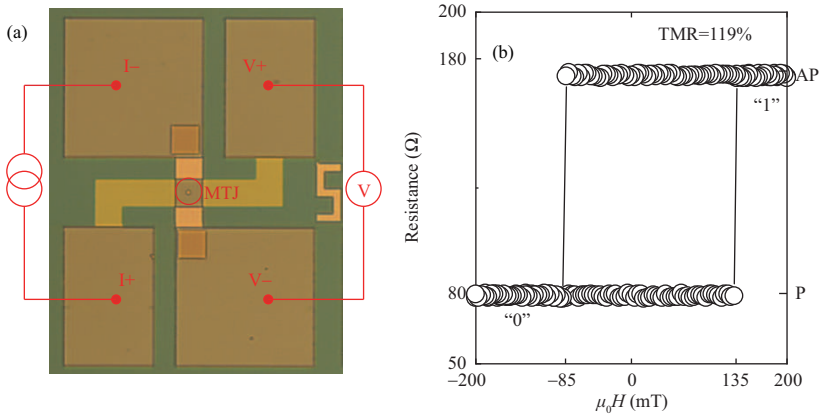

Figure 2 (Color online) Characterization of the fabricated p-DMTJ device. (a) Optical microscope image of the p-DMTJ device. Circular MTJ pillars were fabricated using multistep optical lithography and Ar ion milling. The diameter of the MTJ pillar was 5 μm, with four electrode pads to perform TMR detection. A 100-nm-thick indium tin oxide (ITO) film was employed as the transparent top electrode, enabling both efficient optical access and electrical detection. (b) *R*-*H* magnetoresistance loop measured as a function of applied out-of-plane magnetic field ranging from −200 to +200 mT. The result shows that the double-free layers simultaneously switched, and the TMR ratio was calculated to be 119%.

shows the *M*-*H* hysteresis loops of the p-MTJ film, i.e., without the device fabrication, as a function of the out-of-plane (black) and in-plane (blue) applied magnetic field. The film exhibits that strong PMA was present in both the free and reference layers, as indicated by the 100% remanence and squareness of the major hysteresis loops. According to the minor loop (inset of Figure 1(b)), the two CoFeB FLs simultaneously switched due to the ferromagnetic coupling from the atom-thick W layer, which is critical for the p-DMTJ performance. As reported in our previous work [13], the enhanced annealing endurance, up to 400°C, originates from reduced atom diffusion when a W bridging and spacer layer is used. This improves the crystalline quality of the MgO layer and the bcc texture of the CoFeB layers, resulting in high TMR. Note that the loop shift was relatively small for the full-sheet sample (~ -3 mT), indicating a significant reduction in the stray field attributed to the SAF reference layer. A coercive field of 7 mT was achieved. The anisotropy field was determined from the hard-axis loops by sweeping the in-plane field, and it was found to be as large as 300 mT. These results are consistent with those of previous studies on similar double-FL p-DMTJ stacks.

Furthermore, the full films were used to fabricate circular MTJ pillars using multistep optical lithography and Ar ion milling. A 100-nm-thick ITO layer was used as the transparent top electrode through electron beam evaporation, which allows both efficient optical access and high signal-noise-ratio electrical detection. Because the transparency and electrical conductivity of ITO are significantly dependent on deposition conditions, the deposition process was carefully optimized before the MTJ fabrication, which is a crucial step in laser-assisted switching measurements.

Figure 2(a) shows the optical microscope image of the fabricated MTJ devices with a pillar diameter of 5 μm and four electrode pads for TMR detection.

After fabrication, TMR measurements were performed on the patterned MTJ device by sweeping an out-of-plane magnetic field ranging from −200 to +200 mT, as shown in Figure 2(b). The result shows that the double FLs switched simultaneously, and the MTJs exhibited a bi-resistance state, denoted as $R_{\rm AP} = 173.7\ \Omega$ (AP: antiparallel) and $R_{\rm P} = 79.3\ \Omega$ (P: parallel). Specifically, resistance transition events were observed at the switching field of +135 and −85 mT, which is attributed to the stray field from the Co/Pt SAF layers. The difference in the loop shift between the full-sheet film and patterned MTJ is in agreement with that of the previous studies [11, 13]. The TMR ratio was calculated to be 119%, which could be further enhanced by optimizing the MTJ structure, as reported in previous studies; however, this was beyond the scope of the present work.

3 Results

We further investigated single-pulse fs laser-assisted switching in the p-DMTJ device. In the measurement, the p-DMTJ was first saturated by an external magnetic field. Thereafter, as shown in Figure 3, the p-DMTJ was exposed consecutively to linearly polarized laser pulses with the laser energy of 600 nJ,

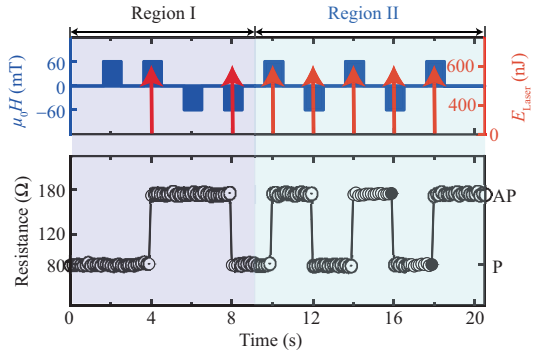

Figure 3 (Color online) Experimental demonstration of fs laser-assisted toggle "write" in the p-DMTJ device. In the measurement, the p-DMTJ was exposed consecutively to linearly polarized laser pulses, which were synchronized with a bipolar out-of-plane magnetic field sequence of ±60 mT. The switching was readout electrically through four-point TMR measurement in real time. In Region I, when only a bipolar magnetic field sequence was applied without firing a laser pulse, both the P and AP states were stable against such a magnetic field disturbance. Switching was only possible when the magnetic field sequence was synchronized by the fs laser pulse train with a pulse energy of 600 nJ. In Region II, robust fs laser-assisted switching of the p-DMTJ was observed, which was determined by the direction of the bipolar magnetic field sequence. The resistance was equal to that in the *R*-*H* loop, indicating a complete reversal. The final resistance state ($R_{\rm P}$, $R_{\rm AP}$) was determined by the direction of the magnetic field sequence ("0" and "1").

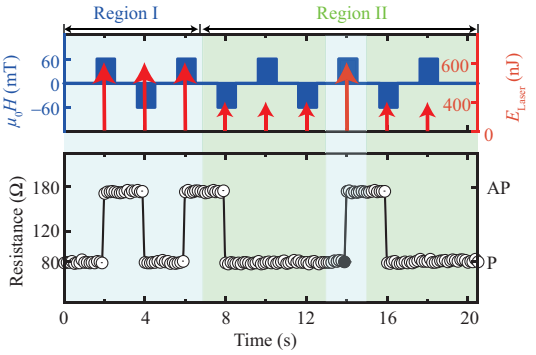

Figure 4 (Color online) Experimental demonstration of fs laser-assisted unidirectional "reset" in the p-DMTJ device. In region I, which was the reference, a magnetic field sequence was synchronized again by the fs laser pulse train with the single-pulse energy of 600 nJ. A reliable toggle switching was also observed. In region II, the laser pulse energy was reduced to 400 nJ. Here, only a unidirectional switching to the P state was observed, and it never toggled back to the AP state using the same configuration. Switching back to AP was only possible with higher laser energy.

which was synchronized with a bipolar out-of-plane magnetic field sequence of ±60 mT (+ and − denoted as "1" and "0", respectively) for a duration of 1 s. The laser pulse duration was ∼ 100 fs, with a spot size of 100 μm and wavelength of 700 nm. The repetition rate of the laser was set to 0.5 Hz to avoid the accumulated heating effect. The magnetoresistance response of the p-DMTJ was measured using a four-point TMR measurement in real time, with a sampling interval of 250 ms.

Figure 3 shows the results of fs laser-assisted switching in the p-DMTJ under different configurations. In region I, which was used as a comparison, in the case when only a bipolar magnetic field sequence was applied without firing a laser pulse, both the P and AP states were stable against such disturbances. Switching was only possible when the magnetic field sequence was synchronized by the fs laser pulse train with the pulse energy of 600 nJ.

As shown in region II, a robust toggle switching of the p-DMTJ upon every fs laser pulse was observed. The fs laser-assisted TMR switching was determined by the direction of the bipolar magnetic field sequence. The resistance was equal to that in the *R*-*H* loop, indicating a complete reversal. The final resistance state ($R_{\rm P}$, $R_{\rm AP}$) was determined by the direction of the magnetic field sequence ("0" and "1"). These results indicate that the proposed laser-assisted writing scheme could be well implemented in p-DMTJ devices because a reliable "write" operation is critical for binary storage devices.

In magnetic storage devices, controllably resetting the memory bit before a "write" operation is often desirable. To validate the unidirectional "reset" operation, the fs laser-assisted switching measurement was performed, as shown in Figure 4. In region I (the reference), the magnetic field sequence was synchronized again by an fs laser pulse train with the single-pulse energy of 600 nJ. A reliable toggle switching to both the AP and P directions was also observed, as shown in Figure 3. In region II, the laser pulse energy was reduced to 400 nJ. Here, only the unidirectional switching to the P state was observed; it never toggled back to the AP state for the same configuration. Switching back to AP was only possible with higher laser energy (600 nJ in our measurements). This asymmetrical switching behavior could be partially attributed to the stray field of the p-DMTJ, which is further discussed in Section 4.

We verified the feasibility of the fs laser-assisted switching in the p-DMTJ. Two proofs-of-concept functionalities, i.e., toggle "write" and unidirectional "reset", were implemented by the interplay of the laser energy and magnetic field sequence. These reconfigurable laser-assisted switching operations indicate an emerging potential for integrated photonic-spintronic storage devices.

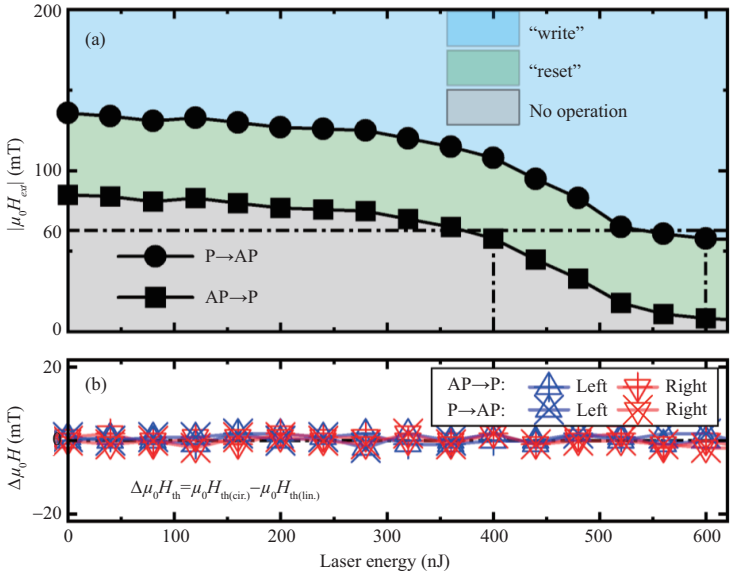

Figure 5 (Color online) Joint effect of the fs laser, magnetic field, and stray filed of p-DMTJ on the proposed switching scheme. (a) Switching phase diagram of fs laser-assisted switching in the p-DMTJs, with the interplay between the fs laser pulse energy and write sequence. Three configuration regimes of the proposed switching scheme are shown. In the case of $|H_{\rm ext}| < |H_{\rm th,AP\to P}|$ (gray region), no successful MTJ switching was observed for both states. In the case of $|H_{\rm ext}| > |H_{\rm th,P\to AP}|$ (blue region), a regime of toggle "write" was observed. For $|H_{\rm th,AP\to P}| < |H_{\rm ext}| < |H_{\rm th,P\to AP}|$ (green region), only the unidirectional AP $\to$ P switching was observed. (b) Typical helicity-dependent measurement for AP $\to$ P and P $\to$ AP switching by fs laser pulse with left- and right-handed circular polarizations, respectively. $\Delta\mu_0 H$ denotes the $|H_{\rm th}|$ deviation relative to the ones for linear polarization. No significant helicity dependence effect was observed using different laser helicity, indicating the major role of conventional TAS induced by laser heating and negligible circular dichroism.

4 Discussion

We further investigated the effect of the laser pulse energy ($E_{\rm p}$), the magnitude of the magnetic field ($|H_{\rm ext}|$), and stray field of the p-DMTJ on the proposed switching scheme. The p-DMTJ device was exposed to a laser pulse train with E_p ranging from 0 to 600 nJ. Thereafter, a synchronized $H_{\rm ext}$ write sequence with the magnitude from 0 to 140 mT was applied. The repetition rate of each measurement was set to 0.1 Hz to avoid accumulative laser heating. The switching was electrically monitored with a real-time TMR measurement.

Figure 5(a) shows the switching phase diagram of the p-DMTJ under the joint effects. For both P $\to$ AP and AP $\to$ P cases, the threshold $|H_{\rm ext}|$ for deterministic switching (denoted as $|H_{\rm th}|$) gradually decreased as the laser energy increased, indicating lowered coercive field. A 92% decrease in $|H_{\rm th,AP\to P}|$ was observed at $E_{\rm p}$ = 600 nJ. The relatively small laser energy to almost fully demagnetize the FL is attributed to an efficient heat transmission of the fs laser pulse compared with current-induced heating in TAS. Furthermore, due to the thermal nature of the proposed scheme, the required laser energy could be scaled down to tens of fJ to write a nanosized MTJ. As already implemented in HAMR technology, using integrated photonic techniques, such as using a nano-photonic plasmonic antenna, a spot radius below 40 nm could be generated [23]. Thus, the proposed scheme shows good potential with enhanced efficiency and scalability.

We observed three configuration regimes of the fs laser-assisted switching scheme, as depicted in Figure 5(a). In the case of $|H_{\rm ext}| < |H_{\rm th,AP\to P}|$ (gray region), no successful MTJ switching was observed for both states. For $|H_{\rm ext}| > |H_{\rm th,P\to AP}|$ (blue region), a regime of binary "write" was observed. These results are consistent with those shown in Figure 3. Moreover, in the case of $|H_{\rm th,AP\to P}| < |H_{\rm ext}| < |H_{\rm th,P\to AP}|$ (green region), only unidirectional AP $\to$ P switching was observed, as shown in Figure 4.

The difference between the $|H_{\rm th,P\to AP}|$ and $|H_{\rm th,AP\to P}|$ demonstrates the asymmetric switching behavior of the proposed scheme, which may be partially attributed to the spatially nonuniformly distributed out-of-plane stray field of the p-DMTJ. The spacing between the two $|H_{\rm th}|$ was almost independent of laser energy, indicating a negligible demagnetization of the reference layer that produces the stray field. Because switching in micro-sized p-MTJ devices is initiated by the domain nucleation and wall propagation, the inhomogeneous distribution of the stray field significantly affects the region where the nucleation

starts [25]. Moreover, the out-of-plane stray field acting on the edges of FLs is much higher than that at the center [25, 26]. Accordingly, lower $H_{\mathrm{th,AP\to P}}$ might be attributed to the stray field that assists nucleation at the edges, and a smaller $|H_{\mathrm{ext}}|$ is needed for complete switching. However, other magnetic interactions, together with the joint effects of ultrafast heating, might also be nontrivial factors causing the asymmetry behavior observed here. Further quantitative investigation on the role of the stray field of p-DMTJs is beyond the scope of the present work. Above all, the combined effects, with the switching phase diagram, provide some insights into the proposed fs laser-assisted switching scheme.

Finally, we investigated if either all-optical helicity-dependent switching (AO-HDS) or magnetic circular dichroism in the PMA layers [27–30] gives rise to significant laser helicity dependence on the p-DMTJ. Previous studies [31] reported that laser-induced helicity-dependent switching can be observed using multiple laser pulses in some of the ferromagnetic systems, such as Co/Pt multilayers and FePt granular media, although not including the CoFeB/MgO system yet. Thus, we consider if significant laser helicity dependence on the CoFeB/MgO-based p-DMTJ exists because it may add functionality for future integrated optospintronic storage applications. To this end, we measured the fs laser-assisted switching in the p-DMTJ using left- and right-handed circularly polarized laser pulses. Figure 5(b) shows the results for AP $\to$ P and P $\to$ AP of the $|H_{\mathrm{th}}|$ deviation compared to the ones using linear polarization. No significant helicity dependence was observed using different laser helicity for switching to both directions, indicating the major role of conventional TAS induced by laser heating and negligible circular dichroism. To enhance the helicity-dependent effect, we propose that material explorations are the first step. By properly designing multilayer stacks or using ferrimagnetic systems such as GdFeCo, the helicity-dependent effect could be enhanced and implemented into device applications, but it was beyond the scope of our present paper.

5 Conclusion

In this study, we experimentally investigated fs laser-assisted switching in a high-performance p-DMTJ device. The feasibility of the proposed scheme was explicitly verified through real time electrical TMR measurements. Notably, reconfigurable laser-assisted switching operations, including binary "write" and unidirectional "reset", were validated using fs laser pulses and synchronized write sequences. Moreover, the joint effects of the laser, magnetic field, and stray field of the p-DMTJ were investigated, and a switching phase diagram was obtained. Negligible laser helicity dependence was also observed, which is attributable to the dominance of thermally-assisted magnetic switching induced by the fs laser pulse. The proposed fs laser-assisted writing scheme for p-DMTJs is promising for future high-density optospintronic storage applications.

Acknowledgements This work was supported in part by National Key R&D Program of China (Grant No. 2018YFB0407602), National Natural Science Foundation of China (Grant No. 61627813), International Collaboration Project (Grant No. B16001), National Key Technology Program of China (Grant No. 2017ZX01032101), Beihang Hefei Innovation Research Institute Project (Grant No. BHKX-19-02), and China Scholarship Council (CSC).

References

1 Kent A D, Worledge D C. A new spin on magnetic memories. Nat Nanotech, 2015, 10: 187–191
2 Zhao W S, Wang Z H, Peng S Z, et al. Recent progresses in spin transfer torque-based magnetoresistive random access memory (STT-MRAM) (in Chinese). Sci Sin-Phys Mech Astron, 2016, 46: 107306
3 Wolf S A, Lu J, Stan M R, et al. The promise of nanomagnetics and spintronics for future logic and universal memory. Proc IEEE, 2010, 98: 2155–2168
4 Chappert C, Fert A, van Dau F N. The emergence of spin electronics in data storage. Nat Mater, 2007, 6: 813–823
5 Puebla J, Kim J, Kondou K, et al. Spintronic devices for energy-efficient data storage and energy harvesting. Commun Mater, 2020, 1: 24
6 Kang W, Huang Y Q, Zhang X C, et al. Skyrmion-electronics: an overview and outlook. Proc IEEE, 2016, 104: 2040–2061
7 Li W-J, Guang Y, Yu G-Q, et al. Skyrmions in magnetic thin film heterostructures. Acta Phys Sin, 2018, 67: 131204
8 Peng S Z, Zhu D Q, Zhou J Q, et al. Modulation of heavy metal/ferromagnetic metal interface for high-performance spintronic devices. Adv Electron Mater, 2019, 5: 1900134
9 Ikeda S, Miura K, Yamamoto H, et al. A perpendicular-anisotropy CoFeB-MgO magnetic tunnel junction. Nat Mater, 2010, 9: 721–724
10 Mangin S, Ravelosona D, Katine J A, et al. Current-induced magnetization reversal in nanopillars with perpendicular anisotropy. Nat Mater, 2006, 5: 210–215
11 Wang M X, Cai W L, Zhu D, et al. Field-free switching of a perpendicular magnetic tunnel junction through the interplay of spin-orbit and spin-transfer torques. Nat Electron, 2018, 1: 582–588
12 Sato H, Yamanouchi M, Ikeda S, et al. MgO/CoFeB/Ta/CoFeB/MgO recording structure in magnetic tunnel junctions with perpendicular easy axis. IEEE Trans Magn, 2013, 49: 4437–4440

13 Wang M X, Cai W L, Cao K H, et al. Current-induced magnetization switching in atom-thick tungsten engineered perpendicular magnetic tunnel junctions with large tunnel magnetoresistance. Nat Commun, 2018, 9: 671
14 Kim J H, Lee J B, An G G, et al. Ultrathin W space layer-enabled thermal stability enhancement in a perpendicular MgO/CoFeB/W/CoFeB/MgO recording frame. Sci Rep, 2015, 5: 16903
15 Zhou J Q, Zhou H Y, Bournel A, et al. Large spin Hall effect and tunneling magnetoresistance in iridium-based magnetic tunnel junctions. Sci China Phys Mech Astron, 2020, 63: 217511
16 Wang L Z, Li X, Sasaki T, et al. High voltage-controlled magnetic anisotropy and interface magnetoelectric effect in sputtered multilayers annealed at high temperatures. Sci China Phys Mech Astron, 2020, 63: 277512
17 Hu G, Lee J H, Nowak J J, et al. STT-MRAM with double magnetic tunnel junctions. In: Proceedings of IEEE International Electron Devices Meeting (IEDM), Washington, 2015. 1–4
18 Kryder M H, Gage E C, McDaniel T W, et al. Heat assisted magnetic recording. Proc IEEE, 2008, 96: 1810–1835
19 Challener W A, Peng C B, Itagi A V, et al. Heat-assisted magnetic recording by a near-field transducer with efficient optical energy transfer. Nat Photon, 2009, 3: 220–224
20 Luo S J, Xu N, Wang Y Y, et al. Thermally assisted Skyrmion memory (TA-SKM). IEEE Electron Device Lett, 2020, 41: 932–935
21 Prejbeanu I L, Kerekes M, Sousa R C, et al. Thermally assisted MRAM. J Phys-Condens Matter, 2007, 19: 165218
22 Prejbeanu I L, Bandiera S, Alvarez-Hérault J, et al. Thermally assisted MRAMs: ultimate scalability and logic functionalities. J Phys D-Appl Phys, 2013, 46: 074002
23 Lalieu M L M, Lavrijsen R, Koopmans B. Integrating all-optical switching with spintronics. Nat Commun, 2019, 10: 110
24 Kimel A V, Li M. Writing magnetic memory with ultrashort light pulses. Nat Rev Mater, 2019, 4: 189–200
25 Gopman D B, Bedau D, Mangin S, et al. Asymmetric switching behavior in perpendicularly magnetized spin-valve nanopillars due to the polarizer dipole field. Appl Phys Lett, 2012, 100: 062404
26 Rietjens J H H, Józsa C, de Jonge W J M, et al. Effect of stray field on local spin modes in exchange-biased magnetic tunnel junction elements. Appl Phys Lett, 2005, 87: 172508
27 Stanciu C D, Hansteen F, Kimel A V, et al. All-optical magnetic recording with circularly polarized light. Phys Rev Lett, 2007, 99: 047601
28 Lalieu M L M, Peeters M J G, Haenen S R R, et al. Deterministic all-optical switching of synthetic ferrimagnets using single femtosecond laser pulses. Phys Rev B, 2017, 96: 220411
29 Beens M, Lalieu M L M, Deenen A J M, et al. Comparing all-optical switching in synthetic-ferrimagnetic multilayers and alloys. Phys Rev B, 2019, 100: 220409
30 Wang L D, van Hees Y L W, Lavrijsen R, et al. Enhanced all-optical switching and domain wall velocity in annealed synthetic-ferrimagnetic multilayers. Appl Phys Lett, 2020, 117: 022408
31 Mangin S, Gottwald M, Lambert C H, et al. Engineered materials for all-optical helicity-dependent magnetic switching. Nat Mater, 2014, 13: 286–292